

Supplementary material

Appendix A: Detailed description of the integrated population model

1. Population model

We developed a female-based, age-structured integrated population model (IPM) of three age classes (i.e., juvenile, yearling, and adult) and a pre-breeding census (Figure A.1).

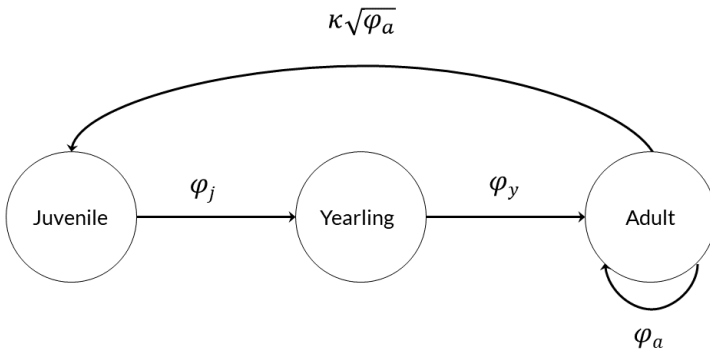


Figure A.1. Age-structured life cycle of the Bewick's swan with juvenile, yearling and adult age classes. φ_x is the annual survival rate between year t and $t+1$ for individuals in age class x , and κ is the apparent breeding success: the average number of female fledglings, per successful breeding female, that survived until first winter.

In the IPM, apparent survival was modelled for juveniles (φ_j), yearlings (φ_y) and adults (φ_a). Resighting probabilities were modelled for leg rings (p_l) and neck bands (p_n) separately, as they are known to have different resighting probabilities (Wood et al., 2018). Because reproduction data from the breeding grounds were lacking, breeding success was modelled through a latent parameter κ . Modelling the age-specific abundances in the IPM with bi-annual time step allowed us to explicitly estimate the actual number of breeding females, and their apparent breeding success, in addition to the number of females in winter. The resulting population transition matrices are as follows:

$$\mathbf{W}_{t+1} = \begin{bmatrix} W_j \\ W_y \\ W_a \end{bmatrix}_{t+1} = \begin{bmatrix} 0 & 0 & \kappa\sqrt{\varphi_a} \\ \varphi_j & 0 & 0 \\ 0 & \varphi_y & \varphi_a \end{bmatrix} \begin{bmatrix} W_j \\ W_y \\ W_a \end{bmatrix}_t \quad (\text{S1.1})$$

which can be separated in the transition from the start of the breeding season to winter,

$$\mathbf{W}_t = \begin{bmatrix} W_j \\ W_y \\ W_a \end{bmatrix}_t = \begin{bmatrix} 0 & 0 & \kappa \\ \sqrt{\varphi_j} & 0 & 0 \\ 0 & \sqrt{\varphi_y} & \sqrt{\varphi_a} \end{bmatrix} \begin{bmatrix} B_j \\ B_y \\ B_a \end{bmatrix}_t \quad (\text{S1.2})$$

and from winter to the start of the breeding season,

$$\mathbf{B}_{t+1} = \begin{bmatrix} B_j \\ B_y \\ B_a \end{bmatrix}_{t+1} = \begin{bmatrix} \sqrt{\varphi_j} & 0 & 0 \\ 0 & \sqrt{\varphi_y} & 0 \\ 0 & 0 & \sqrt{\varphi_a} \end{bmatrix} \begin{bmatrix} W_j \\ W_y \\ W_a \end{bmatrix}_t \quad (\text{S1.3})$$

where $B_{j,t}$, $B_{y,t}$ and $B_{a,t}$ are the number of juveniles, yearlings and adults at the start of the breeding season in year t , respectively, $W_{j,t}$, $W_{y,t}$ and $W_{a,t}$ are the number of juveniles, yearlings and adults in winter in year t , respectively, $\varphi_{x,t}$ is the annual survival probability between t and $t+1$ for individuals in age class x , and κ_t is apparent breeding success, i.e., the average number of female fledglings produced per successful breeding female that survived until first winter in year t .

This model was extended to account for demographic stochasticity, by using binomial and Poisson distributions to link between age-specific numbers in year t and $t+1$, and environmental

35 stochasticity, by allowing annual variation in all demographic rates. The projection matrix
 36 translates to the following relationships:

$$\begin{aligned}
 W_{j,t} & \text{Poisson}(B_{a,t}\kappa_t) \\
 W_{y,t} & \text{Binomial}(\sqrt{\varphi_{j,t}}, B_{j,t}) \\
 W_{a,t} & \text{Binomial}(\sqrt{\varphi_{y,t}}, B_{y,t}) + \text{Binomial}(\sqrt{\varphi_{a,t}}, B_{a,t}) \\
 37 \quad B_{j,t+1} & \text{Binomial}(\sqrt{\varphi_{j,t}}, W_{j,t}) & \text{(S1.4)} \\
 B_{y,t+1} & \text{Binomial}(\sqrt{\varphi_{y,t}}, W_{y,t}) \\
 B_{a,t+1} & \text{Binomial}(\sqrt{\varphi_{a,t}}, W_{a,t})
 \end{aligned}$$

38

39 *II. Likelihoods of the single datasets*

40 Combining the data on the proportion of juveniles (j) and the census data (C), we separated the
 41 counts for juveniles ($C_j = j \cdot C$) and older individuals ($C_{ya} = [1 - j]C$). These two counts were
 42 modelled using state-space models (Brooks et al. 2004). The state-space model consists of a
 43 state process and an observation process. The state process describes the true but unknown
 44 population trajectory under the population model. The observation process describes the link
 45 between the true and the observed population size (De Valpine and Hastings 2002). The state
 46 process models were described in the previous section. For the observation process models we
 47 assumed that the observation error was different between juveniles and older individuals, to
 48 account for the incorporation of the data on the proportion of juveniles, normally distributed on the
 49 log scale and constant over time.

$$\begin{aligned} \log(C_{j,t}) & \sim \text{Normal}(W_{j,t}, \sigma_{j,obs}^2) \\ \log(C_{ya,t}) & \sim \text{Normal}(W_{y,t} + W_{a,t}, \sigma_{ya,obs}^2) \end{aligned} \quad (\text{S1.5})$$

51

52 The likelihood of the state-space model was composed of the likelihood of the observation
53 processes and the state processes (Kéry and Schaub 2011).

54 Capture-mark-resighting data were modelled using a Cormack-Jolly-Seber model (Lebreton et al.
55 1992). We defined the latent variable $z_{i,t}$ as the true state of individual i at time t , which takes
56 value 1 if individual i is alive at time t , and value 0 if individual i is dead at time t . Because only
57 events after first capture are modelled in the CJS model, we also defined vector f_i , which denotes
58 the occasion at which individual i was first captured and marked. The state of individual i at first
59 capture (z_{i,f_i}) is 1 with probability 1. The subsequent occasions are modelled as Bernoulli trials.
60 Conditional on being alive at time t , individual i may survive to time $t+1$ with probability $\phi_{i,t}$,
61 resulting in the following state process model:

$$z_{i,t+1} | z_{i,t} \sim \text{Bernoulli}(z_{i,t} \phi_{i,t}) \quad (\text{S1.6})$$

63

64 If individual i is alive at time t , it may be recaptured/resighted with a probability $p_{i,t}$. With Bernoulli
65 trials, the true state $z_{i,t}$ can be linked to the observation $y_{i,t}$, resulting in the following observation
66 process model:

$$y_{i,t} | z_{i,t} \sim \text{Bernoulli}(z_{i,t} p_{i,t}) \quad (\text{S1.7})$$

68 The probabilities of apparent survival and resighting were modelled with random year effects:

$$\text{logit}(\theta_t) = \bar{\theta} + \varepsilon_{\theta,t} \quad (\text{S1.8})$$

69

70

71 where $\bar{\theta}$ was the mean demographic rate over time on the logit scale and $\varepsilon_{\theta,t}$ the temporal
 72 component of the demographic rate with mean 0 and variance σ_{θ}^2 :

$$73 \quad \varepsilon_{\theta,t} \sim \text{Normal}(0, \sigma_{\theta}^2) \quad (S1.9)$$

74

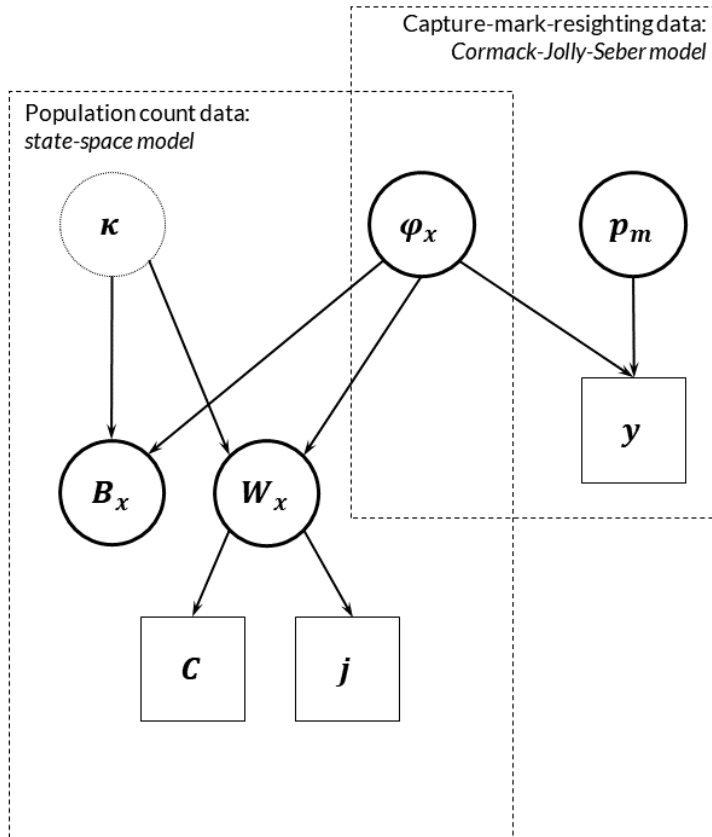
75 *III. Joint likelihood*

76 The joint likelihood of the IPM is the product of the individual likelihoods of the different datasets,
 77 assuming independence between them (Kéry and Schaub 2011). Individuals can appear in
 78 multiple datasets included in this study, so the assumption is violated to some degree. However,
 79 violation of this assumption has been shown to have little effect on estimation of parameters
 80 (Abadi et al. 2010, Schaub and Fletcher 2015), in particular when the number of marked birds is
 81 a small proportion of the studied population (Weegman et al. 2016). The joint likelihood is as
 82 follows:

$$\begin{aligned}
 & L_{IPM}(\mathbf{C}, \mathbf{j}, \mathbf{y} \mid \mathbf{W}_x, \mathbf{B}_x, \boldsymbol{\varphi}_x, \boldsymbol{\kappa}, \mathbf{p}_m, \sigma_{j,obs}^2, \sigma_{ya,obs}^2) = \\
 & L_O(\mathbf{C}, \mathbf{j} \mid \mathbf{W}_x, \sigma_{j,obs}^2, \sigma_{ya,obs}^2) \\
 83 \quad & \times L_S(\mathbf{W}_x, \mathbf{B}_x \mid \boldsymbol{\varphi}_x, \boldsymbol{\kappa}) \quad (S1.10) \\
 & \times L_{CJS}(\mathbf{y} \mid \boldsymbol{\varphi}_x, \mathbf{p}_m)
 \end{aligned}$$

84

85 where L_O is the likelihood of the census observation process model, L_S the likelihood of the census
 86 state process model, L_{CJS} the likelihood of the CJS model, x age class (i.e., juvenile, yearling,
 87 adult) and m mark type (i.e., leg ring, neck band). A graphical representation of this model is
 88 shown in Figure A.2.



89
 90 **Figure A.2.** Directed acyclic graph of the integrated population model. Estimated parameters are
 91 represented by circles, data by rectangles. Arrows represent dependencies between nodes. c
 92 population census data, j proportion of juveniles, y capture-mark-resighting data, W_x is
 93 abundance of age class x (i.e., juvenile, yearling, adult) in winter, B_x is abundance of age class x
 94 in the breeding season, φ_x is the survival probability of age class x , p_m is the resighting probability
 95 of mark type m (i.e., leg ring, neck band), and κ is the latent parameter apparent breeding
 96 success.

97

98 IV. Computation

99 To estimate the parameters, we analysed the joint likelihood combined with prior distributions to
 100 obtain posterior distributions. For all but apparent breeding success, which prior was informed by
 101 the winter brood size, we specified non-informative priors (Table S1). Markov chain Monte Carlo
 102 (MCMC) methods were used to simulate observations from the posterior distributions with JAGS
 103 version 4.3.0 (Plummer 2003) run from R with *jagsUI* version 1.5.1 (Kellner 2019). We ran 3
 104 chains of 200,000 iterations with a burn-in of 100,000, thinning every 50th iteration, resulting in a

105 total of 6,000 posterior samples. Convergence of the MCMC chains was evaluated by ensuring
 106 that the Brooks-Rubin-Gelman diagnostic \hat{R} (Brooks and Gelman 1998) for each parameter was
 107 below 1.1. R and JAGS code of the IPM can be found in Appendix B.

108

109 **Table A.1.** Prior distributions for the parameters in the integrated population model.

Parameter	Prior distribution
Mean survival	$\bar{\varphi}_{j,t} \sim Normal(0,100)T(-5,5)$ $\bar{\varphi}_{y,t} \sim Normal(0,100)T(-5,5)$ $\bar{\varphi}_{a,t} \sim Normal(0,100)T(-5,5)$
Temporal variability of survival	$\varepsilon_{\varphi_j} \sim Normal(0, \sigma_{\varphi_j}^2)$ $\varepsilon_{\varphi_y} \sim Normal(0, \sigma_{\varphi_y}^2)$ $\varepsilon_{\varphi_a} \sim Normal(0, \sigma_{\varphi_a}^2)$ $\sigma_{\varphi_j} \sim Uniform(0,10)$ $\sigma_{\varphi_y} \sim Uniform(0,10)$ $\sigma_{\varphi_a} \sim Uniform(0,10)$
Mean resighting probabilities	$\bar{p}_{l,t} \sim Normal(0,100)T(-5,5)$ $\bar{p}_{n,t} \sim Normal(0,100)T(-5,5)$
Temporal variability of resighting probabilities	$\varepsilon_{p_l} \sim Normal(0, \sigma_{p_l}^2)$ $\varepsilon_{p_n} \sim Normal(0, \sigma_{p_n}^2)$ $\sigma_{p_l} \sim Uniform(0,10)$ $\sigma_{p_n} \sim Uniform(0,10)$
Apparent breeding success (upper limit informed by average winter brood size (Wood et al. 2016))	$\kappa_t \sim Uniform(0,2)$
Observation errors census data	$\sigma_{j,obs} \sim Uniform(0,100)$ $\sigma_{ya,obs} \sim Uniform(0,100)$

Abundances in the breeding season in the first year.

$$B_{j,1} \sim \text{Normal}(300, 10^4) T(0,)$$

$$B_{y,1} \sim \text{Normal}(1000, 10^4) T(0,)$$

$$B_{a,1} \sim \text{Normal}(4000, 10^4) T(0,)$$

110

111 **References Appendix A**

- 112 Abadi, F., Gimenez, O., Arlettaz, R. and Schaub, M. 2010. An assessment of integrated
113 population models: bias, accuracy, and violation of the assumption of independence. -
114 Ecology 91: 7–14.
- 115 Brooks, S. P. and Gelman, A. 1998. General methods for monitoring convergence of iterative
116 simulations. - J. Comput. Graph. Stat. 7: 434–455.
- 117 Brooks, S. P., King, R. and Morgan, B. J. T. 2004. A Bayesian approach to combining animal
118 abundance and demographic data. - Anim. Biodivers. Conserv. 27: 515–529.
- 119 de Valpine, P. and Hastings, A. 2002. Fitting population models incorporating process noise and
120 observation error. - Ecol. Monogr. 72: 57–76.
- 121 Kellner, K. 2019. jagsUI: a wrapper around rjags to streamline JAGS analyses. - R Packag.
122 version 1.5.1. <https://CRAN.R-project.org/package=jagsUI>.
- 123 Kéry, M. and Schaub, M. 2012. Bayesian Population Analysis using WinBUGS. A hierarchical
124 perspective. - Academic Press.
- 125 Lebreton, J.-D., Burnham, K. P., Clobert, J. and Anderson, D. R. 1992. Modeling survival and
126 testing biological hypotheses using marked animals: a unified approach with case studies. -
127 Ecol. Monogr. 62: 67–118.
- 128 Plummer, M. 2003. JAGS: a program for analysis of Bayesian graphical models using Gibbs
129 sampling. - Proc. 3rd Int. Work. Distrib. Stat. Comput. Vienna, Austria.
- 130 Rees, E. C. 2006. Bewick's Swan. - T. & A.D. Poyser.
- 131 Schaub, M. and Fletcher, D. 2015. Estimating immigration using a Bayesian integrated
132 population model: choice of parametrization and priors. - Environ. Ecol. Stat. 22: 535–549.
- 133 Weegman, M. D., Bearhop, S., Fox, A. D., Hilton, G. M., Walsh, A. J., McDonald, J. L. and
134 Hodgson, D. J. 2016. Integrated population modelling reveals a perceived source to be a
135 cryptic sink. - J. Anim. Ecol. 85: 467–475.
- 136 Wood, K. A., Newth, J. L., Hilton, G. M., Nolet, B. A. and Rees, E. C. 2016. Inter-annual
137 variability and long-term trends in breeding success in a declining population of migratory
138 swans. - J. Avian Biol. 47: 1–13.
- 139 Wood, K. A., Nuijten, R. J. M., Newth, J. L., Haitjema, T., Vangeluwe, D., Ioannidis, P., Harrison,
140 A. L., Mackenzie, C., Hilton, G. M., Nolet, B. A. and Rees, E. C. 2018. Apparent survival of
141 an Arctic-breeding migratory bird over 44 years of fluctuating population size. - Ibis 160:
142 413–430.

143

144 **Appendix B: R and JAGS code for the integrated population model**

145

```
146 # Data objects
147
148 # eh: encounter history matrix
149 # f: vector of first observations
150 # x: age matrix
151 # juvper: proportion of juveniles in winter
152 # counts: population winter counts
153 # gr: leg ring vs neck band
154
155 sink("ipm-season-s3.jags")
156 cat("
157     model {
158
159         #*****
160         # 1. Define priors and constraints
161         #*****
162
163         #*****
164         # 1.1 Initial population sizes
165         #*****
166         b1 ~ dnorm(300, 0.001)T(0,) # Number of 1-year olds in breeding
167         season
168         b2 ~ dnorm(1000, 0.001)T(0,) # Number of 2-year olds in breeding
169         season
170         b3 ~ dnorm(4000, 0.001)T(0,) # Number of 3-year olds and older in
171         breeding season
172
173         B1[1] <- round(b1)
174         B2[1] <- round(b2)
175         B3[1] <- round(b3)
176
177         #*****
178         # 1.2 Observation errors
179         #*****
180         sigma.y ~ dunif(0, 100)
181         sigma2.y <- pow(sigma.y, 2)
182         tauy <- pow(sigma.y, -2) # Precision counts 1.5-year olds and
183         older
184
185         sigma.z ~ dunif(0, 100)
186         sigma2.z <- pow(sigma.z, 2)
187         tauz <- pow(sigma.z, -2) # Precision counts 0.5-year olds
188
189         #*****
190         # 1.3 Survival probabilities (3 age classes)
191         #*****
192         for(a in 1:3){
193             for(t in 1:(nyears-1)){
```

```

194     eta.phi[a,t] <- mu.phi[a] + epsilon.phi[a,t]
195     epsilon.phi[a,t] ~ dnorm(0, tau.phi[a])T(-15,15)
196   } #t
197   mu.phi[a] ~ dnorm(0, 0.01)T(-5,5)
198   sigma.phi[a] ~ dunif(0, 10)
199   tau.phi[a] <- pow(sigma.phi[a], -2)
200   sigma2.phi[a] <- pow(sigma.phi[a], 2)
201 } #a
202
203 # Constrain parameters
204 for(i in 1:nind){
205   for(t in f[i]:(nyears-1)){
206     logit(phi[i,t]) <- eta.phi[x[i,t],t]
207   } #t
208 } #i
209
210 #*****
211 # 1.3 Resighting probabilities (2 classes)
212 #*****
213 for(g in 1:2){ # leg rings and neck bands
214   for(t in 1:(nyears-1)){
215     eta.p[g,t] <- mu.p[g] + epsilon.p[g,t]
216     epsilon.p[g,t] ~ dnorm(0, tau.p[g])T(-15,15)
217   } #t
218   mu.p[g] ~ dnorm(0, 0.01)T(-5,5)
219   sigma.p[g] ~ dunif(0, 10)
220   tau.p[g] <- pow(sigma.p[g], -2)
221   sigma2.p[g] <- pow(sigma.p[g], 2)
222 } #g
223
224 # Constrain parameters
225 for(i in 1:nind){
226   for(t in f[i]:(nyears-1)){
227     logit(p[i,t]) <- eta.p[group[i],t]
228   } #t
229 } #i
230
231 #*****
232 # 1.4 Apparent breeding success
233 #*****
234 for(t in 1:nyears){
235   kappa[t] ~ dunif(0, 2) # Informed by winter brood size
236 } #t
237
238 #*****
239 # 1.5 Derived parameters
240 #*****
241
242 # Survival
243 for(t in 1:(nyears-1)){
244   logit(phi.j[t]) <- eta.phi[1,t]
245   logit(phi.y[t]) <- eta.phi[2,t]

```

```

246     logit(phi.a[t]) <- eta.phi[3,t]
247   } #t
248
249   # Resighting
250   for(t in 1:(nyears-1)){
251     logit(p.l[t]) <- eta.p[1,t]
252     logit(p.n[t]) <- eta.p[2,t]
253   } #t
254
255   #*****
256   # 2 Likelihoods of single datasets
257   #*****
258
259   #*****
260   # 2.1 Population count data (state-space model)
261   #*****
262
263   # 2.1.1 System process
264   for (t in 1:(nyears-1)){
265     B1[t+1] ~ dbin(phi.j[t]^(1/2), W1[t])
266     B2[t+1] ~ dbin(phi.y[t]^(1/2), W2[t])
267     B3[t+1] ~ dbin(phi.a[t]^(1/2), W3[t])
268   } #t
269
270   for (t in 1:(nyears-1)){
271     mean.w[t] <- B3[t] * kappa[t]
272     W1[t] ~ dpois(mean.w[t])
273     W2[t] ~ dbin(phi.j[t]^(1/2), B1[t])
274     W3a[t] ~ dbin(phi.y[t]^(1/2), B2[t])
275     W3b[t] ~ dbin(phi.a[t]^(1/2), B3[t])
276     W23[t] <- W2[t] + W3a[t] + W3b[t]
277     W3[t] <- W3a[t] + W3b[t]
278   } #t
279
280   # 2.1.2 Observation process
281   for (t in 1:(nyears-1)){
282     cen[t] ~ dnorm(W23[t], tauy)
283     cenjuv[t] ~ dnorm(W1[t], tauz)
284   } #t
285
286   #*****
287   # 2.2 Capture-mark-resighting data (CJS model)
288   #*****
289
290   for(i in 1:nind){
291     # Define latent state at first capture
292     z[i,f[i]] <- 1
293     for (t in (f[i]+1):nyears){
294       # State process
295       z[i,t] ~ dbern(mul[i,t])
296       mul[i,t] <- phi[i,t-1] * z[i,t-1]
297       # Observation process

```

```

298     y[i,t] ~ dbern(mu2[i,t])
299     mu2[i,t] <- p[i,t-1] * z[i,t]
300   } #t
301   } #i
302
303   }
304   ",fill = TRUE)
305 sink()
306
307
308 # Bundle data
309 jags.data.season.s3 <-
310   list(
311     y = eh,
312     f = f,
313     x = x,
314     z = known.state.cjs(eh),
315     nind = dim(eh)[1],
316     nyears = dim(eh)[2],
317     cen = round((1 - juvper/100) * counts/2),
318     cenjuv = round(juvper/100 * counts/2),
319     group = gr
320   )
321
322 # Initial values
323 inits.season.s3 <-
324   function() {
325     list(
326       z = cjs.init.z(eh, f),
327       epsilon.phi = array(0, dim = c(3, dim(eh)[2] - 1)),
328       epsilon.p = array(0, dim = c(2, dim(eh)[2] - 1)),
329       mu.phi = runif(3, 0.01, 1),
330       mu.p = runif(2, 0.01, 1),
331       kappa = runif(dim(eh)[2] - 1, 0.01, 2),
332       sigma.phi = runif(3, 0.1, 10),
333       sigma.p = runif(2, 0.1, 10),
334       sigma.y = runif(1, 0.1, 10),
335       sigma.z = runif(1, 0.1, 10),
336       b1 = rpois(1, 300),
337       b2 = rpois(1, 2000),
338       b3 = rpois(1, 3000)
339     )
340   }
341
342 # Parameters to be monitored
343 parameters.season.s3 <- c("phi.j", "phi.y", "phi.a", "p.l", "p.n",
344 "kappa", "B1", "B2", "B3", "W1", "W2", "W3", "W23", "sigma2.phi",
345 "sigma2.p", "sigma2.y", "sigma2.z")

```

```
346
347 # MCMC settings
348 ni <- 200000
349 nt <- 50
350 nb <- 100000
351 nc <- 3
352
353 # Run model with jagsUI
354 ipm.season.s3 <-
355   jags(
356     jags.data.season.s3,
357     inits.season.s3,
358     parameters.season.s3,
359     "ipm-season-s3.jags",
360     n.chains = nc,
361     n.thin = nt,
362     n.iter = ni,
363     n.burnin = nb
364   )
365
366
```

367 **Appendix C: Transient life table response experiment**

368

369 To calculate the contributions of demographic parameters and components of the population
 370 structure to the population dynamics, we performed a transient life table response experiment
 371 (transient LTRE) based on developments by Caswell (2007) and Koons et al. (2016, 2017).

372 For a time-varying population matrix model \mathbf{A}_t , the realized population growth rate at any time
 373 step can be expressed as:

$$374 \quad \lambda_t = \hat{\mathbf{n}}_{t+1} / \hat{\mathbf{n}}_t = \mathbf{A}_t \hat{\mathbf{n}}_t / \hat{\mathbf{n}}_t \quad (\text{S1.11})$$

375 where $\hat{\mathbf{n}}_{t+1}$ and $\hat{\mathbf{n}}_t$ are vectors of structured population abundances at time $t+1$ and t , respectively.

376 To decompose the variance in λ_t into contributions from the variance in underlying demographic
 377 parameters and components of the population structure, we first expanded eq. S3.1 for our age-
 378 structured population model:

$$379 \quad \lambda_t = \frac{\sqrt{\varphi_{a,t}} \cdot \kappa_t \cdot \hat{w}_{a,t} + \varphi_{j,t} \cdot \hat{w}_{j,t} + \varphi_{y,t} \cdot \hat{w}_{y,t} + \varphi_{a,t} \cdot \hat{w}_{a,t}}{\hat{w}_{j,t} + \hat{w}_{y,t} + \hat{w}_{a,t}}$$

$$380 \quad (\text{S1.12})$$

381 where $\hat{w}_{j,t}$, $\hat{w}_{y,t}$ and $\hat{w}_{a,t}$ are the number of juveniles, yearlings and adults in winter in year t ,
 382 respectively, $\varphi_{x,t}$ is the annual apparent survival rate between t and $t+1$ for individuals in age
 383 class x , and κ_t is the annual apparent breeding success. Each demographic parameter (i.e., each
 384 element of \mathbf{A}_t) and each component of the population structure (i.e., each element of \mathbf{w}_t) is
 385 combined in a vector Θ_t . Contrary to Koons et al. (2016), but in line with Layton-Matthews et al.
 386 (2019), we used non-normalized values for the components of the population structure because
 387 actual rather than relative abundances more appropriately represent possible density dependent
 388 consequences for the population dynamics. Next, we calculated the sensitivity of λ_t to change in

389 each element of Θ_t , which are the first derivatives of λ_t with respect to changes in each element
 390 of Θ_t

$$\begin{aligned}
 \frac{\partial \lambda_t}{\partial \kappa_t} &= \frac{\sqrt{\varphi_{a,t}} \cdot \hat{w}_{a,t}}{\mathbf{w}_t} \\
 \frac{\partial \lambda_t}{\partial \varphi_{j,t}} &= \frac{\hat{w}_{j,t}}{\mathbf{w}_t} \\
 \frac{\partial \lambda_t}{\partial \varphi_{y,t}} &= \frac{\hat{w}_{y,t}}{\mathbf{w}_t} \\
 \frac{\partial \lambda_t}{\partial \varphi_{a,t}} &= \frac{\hat{w}_{a,t}}{\mathbf{w}_t} \cdot \left(1 + \frac{\kappa_t}{2\sqrt{\varphi_{a,t}}} \right) \\
 \frac{\partial \lambda_t}{\partial \hat{w}_{j,t}} &= \frac{\varphi_{j,t} \cdot \mathbf{w}_t - \mathbf{w}_{t+1}}{\mathbf{w}_t^2} \\
 \frac{\partial \lambda_t}{\partial \hat{w}_{y,t}} &= \frac{\varphi_{y,t} \cdot \mathbf{w}_t - \mathbf{w}_{t+1}}{\mathbf{w}_t^2} \\
 \frac{\partial \lambda_t}{\partial \hat{w}_{a,t}} &= \frac{(\kappa_t \sqrt{\varphi_{a,t}} + \varphi_{a,t}) \cdot \mathbf{w}_t - \mathbf{w}_{t+1}}{\mathbf{w}_t^2}
 \end{aligned} \tag{S1.13}$$

392 where \mathbf{w}_t is the denominator of eq. S3.2, i.e., $\mathbf{w}_t = \hat{w}_{j,t} + \hat{w}_{y,t} + \hat{w}_{a,t}$, and \mathbf{w}_{t+1} the numerator of eq.
 393 S1.2, i.e., $\mathbf{w}_{t+1} = \sqrt{\varphi_{a,t}} \cdot \kappa_t \cdot \hat{w}_{a,t} + \varphi_{j,t} \cdot \hat{w}_{j,t} + \varphi_{y,t} \cdot \hat{w}_{y,t} + \varphi_{a,t} \cdot \hat{w}_{a,t}$. Sensitivities were evaluated at the
 394 mean values of each element in Θ_t across the time series. These sensitivities were then combined
 395 with the covariances among all elements of Θ to achieve the first-order approximation of the
 396 variance in λ_t . The contribution of variation in each element of Θ to $\text{var}(\lambda_t)$ was obtained by
 397 summing over the covariances (Horvitz et al. 1997):

398

$$\text{contribution}_{\theta_i}^{\text{var}(\lambda_t)} \approx \sum_j \text{cov}(\theta_{i,t}, \theta_{j,t}) \frac{\partial \lambda_t}{\partial \theta_{i,t}} \frac{\partial \lambda_t}{\partial \theta_{j,t}} \bigg|_{\bar{\theta}} \quad (\text{S1.14})$$

399 Results of the LTRE are visualized in Figure 2 in the main text and Table C.1. Relative
 400 contribution and relative absolute contribution of vital rates to variation in population growth rate
 401 was 106% and 94%, respectively, whilst the population structure contributed -6% and 6%,
 402 respectively.

403

404 **Table C.1.** Estimated variance, sensitivities of realized population growth rate to changes in
 405 underlying vital rates and population structure components, transient life table response
 406 experiment (LTRE) contributions (eq. S3.4), relative contributions (
 407 $\text{contribution}_{\theta_i}^{\text{var}(\lambda_t)} / \sum_i \text{contribution}_{\theta_i}^{\text{var}(\lambda_t)}$) and relative absolute contributions (
 408 $\text{abs}(\text{contribution}_{\theta_i}^{\text{var}(\lambda_t)}) / \sum_i \text{abs}(\text{contribution}_{\theta_i}^{\text{var}(\lambda_t)})$) to variation in realized population growth
 409 rates. Estimates are provided as posterior means and 95% credible intervals.

Parameter	Variance	Sensitivity	LTRE contribution	Relative contribution	Relative absolute contribution
κ	0.0066	0.7159 (0.7110, 0.7211)	0.0034 (0.0029, 0.0038)	0.521 (0.457, 0.592)	0.461 (0.409, 0.516)
φ_j	0.0059	0.1225 (0.1204, 0.1246)	0.0002 ($1.116 \cdot 10^{-5}$, 0.0005)	0.033 (0.002, 0.072)	0.029 (0.003, 0.063)
φ_y	0.0004	0.1116 (0.1092, 0.1140)	0.0001 ($-2.667 \cdot 10^{-5}$, 0.0002)	0.010 (-0.004, 0.033)	0.009 (0.000, 0.029)
φ_a	0.0034	0.8417 (0.8388, 0.8445)	0.0032 (0.0025, 0.0041)	0.501 (0.437, 0.560)	0.444 (0.381, 0.501)
w_j	$1.987 \cdot 10^5$	$-1.102 \cdot 10^{-5}$ ($-1.281 \cdot 10^{-5}$, $-9.321 \cdot 10^{-6}$)	-0.0002 (-0.0003, -0.0002)	-0.032 (-0.040, -0.026)	0.029 (0.023, 0.035)
w_y	$2.085 \cdot 10^5$	$-8.287 \cdot 10^{-6}$ ($-1.026 \cdot 10^{-6}$, $-6.502 \cdot 10^{-6}$)	-0.0001 (-0.0001, -0.0001)	-0.012 (-0.017, -0.008)	0.011 (0.007, 0.015)
w_a	$5.135 \cdot 10^6$	$2.972 \cdot 10^{-6}$ ($2.649 \cdot 10^{-6}$, $-3.316 \cdot 10^{-6}$)	-0.0001 (-0.0002, -0.0001)	-0.020 (-0.025, -0.016)	0.018 (0.015, 0.022)

410

411

412

413 **References Appendix C**

- 414 Caswell, H. 2007. Sensitivity analysis of transient population dynamics. - *Ecol. Lett.* 10: 1–15.
- 415 Horvitz, C., Schemske, D. W. and Caswell, H. 1997. The relative “importance” of life-history
416 stages to population growth: prospective and retrospective analyses. - In: Tuljapurkar, S.
417 and Caswell, H. (eds), *Structured-Population Models in Marine, Terrestrial and Freshwater*
418 *Systems*. Chapman and Hall, New York, NY, pp. 247–271.
- 419 Koons, D. N., Iles, D. T., Schaub, M. and Caswell, H. 2016. A life-history perspective on the
420 demographic drivers of structured population dynamics in changing environments. - *Ecol.*
421 *Lett.* 19: 1023–1031.
- 422 Koons, D. N., Arnold, T. W. and Schaub, M. 2017. Understanding the demographic drivers of
423 realized population growth rates. - *Ecol. Appl.* 27: 2102–2115.
- 424 Layton-Matthews, K., Loonen, M. J. J. E., Hansen, B. B., Coste, C. F. D., Sæther, B. E. and
425 Grøtan, V. 2019. Density-dependent population dynamics of a high Arctic capital breeder,
426 the barnacle goose. - *J. Anim. Ecol.* 88: 1–11.
- 427
- 428

429 **Appendix D**

430

431 **Table D.1.** Pearson correlations between original explanatory variables Year, Whooper swan estimate,
 432 Tailwind, Lake Peipsi water level, negative degree days (nnd) Naryan-Mar, cumulative degree days (cdd)
 433 Naryan-Mar and Bewick's swan estimate.

	Year	whooper est.	Tail-wind	Lake Peipsi	nnd	cdd	Bewick's est.
Year	1	0.959	-0.047	-0.132	0.134	0.281	0.575
whooper est.	0.959	1	0.005	-0.165	0.211	0.231	0.591
Tailwind	-0.047	0.005	1	0.080	-0.054	-0.121	0.002
Lake Peipsi	-0.132	-0.165	0.008	1	-0.244	-0.065	0.042
nnd Narjan	0.134	0.211	-0.054	-0.244	1	0.274	0.045
cdd Narjan	0.281	0.231	-0.121	-0.065	0.274	1	0.016
Bewick's est.	0.575	0.591	0.002	0.042	0.045	0.016	1

434

435 **Table D.2.** AIC values of the different GLM models with demographic parameters as response variables
 436 (columns) and environmental variables as predictors. The three different models are indicated by their
 437 unique predictors (year, whooper swan estimate and Bewick's swan estimate) as these only occur in one
 438 of the models. The other predictor variables (see Table D.1) are present in all three models. Where the
 439 differences in AIC values are >2, models are not considered different.

	Adult survival	Yearling survival	Juvenile survival	Kappa
Year	116.19	108.73	100.11	108.18
whooper swan estimate	116.18	108.74	103.70	108.11
Bewick's swan estimate	115.38	104.27	104.18	110.26

440

441 **Table D.3.** Model output of GLM with demographic parameters estimated by the IPM as response variables
 442 (adult, yearling and juvenile survival, and apparent breeding success) and the explanatory variables as
 443 predictors (Year, Whooper swan estimate, Bewick's swan estimate, Tailwind in the Baltic sea in autumn,
 444 water level in Lake Peipsi in autumn, negative degree days in Naryan-Mar in spring, cumulative degree
 445 days in Naryan-Mar in summer and autumn combined). Because Year, Whooper swan estimate and
 446 Bewick's swan estimate correlate strongly, we only included one of them in a separate model. Table A
 447 shows the results of the GLM with year, B shows the results of the GLM with Whooper swan estimates, C
 448 shows the results of the GLM with Bewick's swan estimates. For adult survival and yearling survival, the
 449 model with Bewick's swan estimates was the most parsimonious (see Table D.1.), for juvenile survival and
 450 kappa the model with year was the most parsimonious (see Table D.1). These results are therefore
 451 presented in the main text.

452

453

454

455 A

456 ~ year + Tailwind + Lake Peipsi water level + ndd Narjan Mar + cdd Narjan Mar

	Adult survival				Yearling survival				Juv. survival				Apparent breeding success			
	Est	SE	t	P	Est	SE	t	P	Est	SE	t	P	Est	SE	t	P
(Intercept)	-0.146	0.175	-0.837	0.409	0.015	0.158	0.099	0.922	-0.070	0.141	-0.498	0.622	0.057	0.157	0.363	0.719
Year	0.090	0.198	0.453	0.654	0.013	0.179	0.075	0.940	0.584	0.160	3.660	0.001	-0.560	0.178	-3.149	0.004
Tailwind	0.148	0.167	0.875	0.388	0.006	0.153	0.037	0.971	0.208	0.137	1.529	0.136	0.027	0.152	0.179	0.859
Lake Peipsi	0.259	0.173	1.490	0.146	0.205	0.157	1.309	0.200	0.426	0.140	3.049	0.005	-0.092	0.156	-0.591	0.559
ndd Narjan	0.165	0.208	0.793	0.434	0.063	0.188	0.336	0.739	0.344	0.168	2.051	0.049	0.030	0.187	0.161	0.873
cdd Narjan	-0.164	0.183	-0.895	0.378	-0.210	0.166	-1.267	0.215	-0.167	0.148	-1.130	0.267	0.046	0.164	0.282	0.780

457

458 B

459 ~ Whooper swan estimate + Tailwind + Lake Peipsi water level + ndd Narjan Mar + cdd Narjan Mar

	Adult survival				Yearling survival				Juv. survival				Apparent breeding success			
	Est	SE	t	P	Est	SE	t	P	Est	SE	t	P	Est	SE	t	P
(Intercept)	-0.144	0.175	-0.827	0.415	0.016	0.158	0.104	0.917	-0.054	0.147	-0.364	0.718	0.044	0.156	0.282	0.780
whooper est.	0.087	0.187	0.463	0.647	0.000	0.170	0.003	0.998	0.484	0.159	3.049	0.005	-0.533	0.168	-3.161	0.004
Tailwind	0.144	0.170	0.850	0.402	0.006	0.154	0.036	0.971	0.186	0.143	1.298	0.204	0.052	0.152	0.342	0.734
Lake Peipsi	0.259	0.174	1.490	0.145	0.203	0.157	1.297	0.204	0.420	0.147	2.864	0.007	-0.096	0.156	-0.619	0.540
ndd Narjan	0.156	0.210	0.745	0.462	0.063	0.190	0.335	0.740	0.295	0.177	1.664	0.106	0.086	0.188	0.457	0.651
cdd Narjan	-0.159	0.180	-0.881	0.385	-0.207	0.163	-1.267	0.215	-0.116	0.152	-0.762	0.452	0.012	0.162	0.071	0.944

460

461 C

462 ~ Bewick's swan estimate + Tailwind + Lake Peipsi water level + ndd Narjan Mar + cdd Narjan Mar

	Adult survival				Yearling survival				Juv. survival				Apparent breeding success			
	Est	SE	t	P	Est	SE	t	P	Est	SE	t	P	Est	SE	t	P
(Intercept)	-0.150	0.173	-0.867	0.393	-0.000	0.149	-0.001	1.0	-0.058	0.149	-0.390	0.699	0.047	0.161	0.290	0.774
Tailwind	0.148	0.168	0.885	0.383	0.005	0.144	0.038	0.970	0.208	0.144	1.447	0.158	0.027	0.157	0.174	0.862
Lake Peipsi	0.238	0.170	1.402	0.171	0.188	0.146	1.282	0.209	0.328	0.146	2.242	0.032	0.003	0.159	0.022	0.983
ndd Narjan	0.156	0.206	0.756	0.455	0.043	0.178	0.245	0.808	0.326	0.177	1.839	0.075	0.049	0.193	0.253	0.802
cdd Narjan	-0.141	0.175	-0.807	0.426	-0.206	0.150	-1.368	0.181	-0.017	0.150	-0.115	0.909	-0.097	0.163	-0.597	0.555
Bewick's est.	0.174	0.183	0.949	0.350	0.315	0.158	1.995	0.055	0.466	0.157	2.962	0.006	-0.474	0.171	-2.772	0.009

463

464

465